THE JOURNAL OF BIOLOGICAL CHEMISTRY VOL. 286, NO. 26, pp. 22833–22845, July 1, 2011

Chloride Channel (Clc)-5 Is Necessary for Exocytic Trafficking of Na^+/H^+ Exchanger 3 (NHE3)*[S]

Received for publication, January 26, 2011, and in revised form, April 6, 2011 Published, JBC Papers in Press, May 11, 2011, DOI 10.1074/jbc.M111.224998

Zhihong Lin[‡1], Shi Jin[‡1], Xiaohong Duan[‡2], Tong Wang[§], Sabrina Martini[‡3], Phuson Hulamm[‡], Boyoung Cha[‡], Ann Hubbard[¶], Mark Donowitz[‡‖4], and Sandra E. Guggino[‡‖]

From the Departments of [‡]Medicine, [‖]Physiology, and [¶]Cell Biology, The Johns Hopkins University School of Medicine, Baltimore, Maryland 21205 and [§]Department of Physiology, Yale University School of Medicine, New Haven, Connecticut 06520

ClC-5, a chloride/proton exchanger, is predominantly expressed and localized in subapical endosomes of the renal proximal tubule. Mutations of the *CLCN5* gene cause Dent disease. The symptoms of Dent disease are replicated in *Clcn5* knock-out mice. Absence of ClC-5 in mice is associated with reduced surface expression of NHE3 in proximal tubules. The molecular basis for this change is not fully understood. In this study, we investigated the mechanisms by which ClC-5 regulates trafficking of NHE3. Whether ClC-5-dependent endocytosis, exocytosis, or both contributed to the altered distribution of NHE3 was examined. First, NHE3 activity in proximal tubules of wild type (WT) and *Clcn5* KO mice was determined by two-photon microscopy. Basal and dexamethasone-stimulated NHE3 activity of *Clcn5* KO mice was decreased compared with that seen in WT mice, whereas the degree of inhibition of NHE3 activity by increasing cellular concentration of cAMP (forskolin) or Ca^{2+} (A23187) was not different in WT and *Clcn5* KO mice. Second, NHE3-dependent absorption of HCO_3^-, measured by single tubule perfusion, was reduced in proximal tubules of *Clcn5* KO mice. Third, by cell surface biotinylation, trafficking of NHE3 was examined in short hairpin RNA (shRNA) plasmid-transfected opossum kidney cells. Surface NHE3 was reduced in opossum kidney cells with reduced expression of ClC-5, whereas the total protein level of NHE3 did not change. Parathyroid hormone decreased NHE3 surface expression, but the extent of decrease and the rate of endocytosis observed in both scrambled and ClC-5 knockdown cells were not significantly different. However, the rates of basal and dexamethasone-stimulated exocytosis of NHE3 were attenuated in ClC-5 knockdown cells. These results show that ClC-5 plays an essential role in exocytosis of NHE3.

Significant information about the function of the intracellular voltage-dependent chloride/proton exchanger ClC-5[5] has come from the characterization of patients with Dent disease and knock-out mouse models of *Clcn5* that have the renal characteristics of this disease (1–5). Dent disease is caused by mutations of *CLCN5* (6–8) and is characterized by low molecular weight proteinuria, aminoaciduria, glycosuria, hyperphosphaturia, hypercalciuria, and sodium and water loss with nephrolithiasis and progressive renal failure (9–11).

ClC-5 is a member of the CLC family of chloride-transporting proteins that includes Cl^- channels and Cl^-/H^+ exchangers (12–16). ClC-5 is expressed in the proximal tubule, the thick ascending limb, and the intercalated cells of the collecting duct in the human nephron (10, 17). In the mouse proximal tubule, immunofluorescence results indicate that ClC-5 is colocalized with the H^+-ATPase, indicating an endosomal location (10, 18). The pH of transferrin-positive endosomes of cultured cells from *Clcn5* knock-out proximal tubule cells is more alkaline than that observed in WT controls (19). The role of ClC-5 is thought to be moving chloride as a counterion to the proton that is pumped by the H^+-ATPase (17, 20, 21), although a role for Cl^- beyond charge has been suggested recently (22).

Detailed studies of trafficking proteins in ClC-5-negative tissues have not been reported. Piwon *et al.* (2) demonstrated that the surface expression of Nhe3 and Npt2a, which are transporters regulated by trafficking and normally reside in the renal proximal tubule brush border membrane, was significantly decreased in the *Clcn5* KO mouse, and total Npt2a expression was decreased. Likewise, the proximal tubule scavenger receptor megalin was decreased in total amount and even further reduced at the apical surface (2, 23). These results suggested that apical domain trafficking was probably abnormal in the *Clcn5* KO proximal tubule. However, no systematic evaluation of the role of ClC-5 in apical domain endocytosis/exocytosis has been reported. In mice fed with a phosphate-depleted diet, parathyroid hormone-induced NHE3 endocytosis was slowed in the *Clcn5* KO proximal tubule, indicating that the endocytosis in intact mice is regulated in a ClC-5-dependent manner (2).

* This work was supported, in whole or in part, by National Institutes of Health Grants PO1 DK72084, RO1 DK26523, RO1 DK61765, R24 DK64388, and P30 DK079310.

[S] The on-line version of this article (available at http://www.jbc.org) contains supplemental Fig. 1.

[1] Both authors are equal contributors to this work.

[2] Present address: Dept. of Oral Biology, School of Stomatology, The Fourth Military Medical University, Xi'an 710032, China.

[3] Supported by Fundacao Carlos Chagas Filho de Amparo a Pesquisa do Estado do Rio de Janeiro and Conselho Nacional de Desenvolvimento Cientifico e Technologico. Present address: Inst. de Biophysica Carlos Chagas, University Federal do Rio De Janeiro, Rio De Janeiro, Brazil 21941.

[4] To whom correspondence should be addressed: Dept. of Medicine, The Johns Hopkins University School of Medicine, 925 Ross Research Bldg., 720 Rutland Ave., Baltimore, MD 21205. Tel.: 410-955-9675; E-mail: mdonowit@jhmi.edu.

[5] The abbreviations used are: ClC, chloride channel; ClC-5, protein in human, mouse, and opossum kidney cell line; *CLCN5*, human gene; *Clcn5*, mouse gene; OK cells, opossum kidney cells; NHE3, Na^+/H^+ exchanger 3; Nhe3, mouse Na^+/H^+ exchange 3; Npt2a, mouse sodium-phosphate cotransporter type IIa; PTH, parathyroid hormone; DEX, dexamethasone; sc, scrambled construct; sh, shRNA; KD, knockdown; BB, brush border; NHS, *N*-hydroxysuccinimide; TMA, tetramethylammonium; ROI, regions of interest; shRNAi, shRNA interference.

However, slowed endocytosis would not explain the decreased steady-state surface distribution of Nhe3 in the *Clcn5* KO proximal tubule. Consequently, Jentsch and co-workers (2) hypothesized that in the *Clcn5* KO mouse this was caused by a high concentration of tubular parathyroid hormone (PTH) caused by decreased reabsorption of PTH via megalin. Based on these observations, we believe that, due to the presence of both primary and secondary effects of ClC-5 in animal models, it may not be possible to fully dissect the direct role of ClC-5 in trafficking of apical membrane proteins by only using animal models. For example, in *Clcn5* KO mice, changed luminal tubule levels of PTH might mask the direct function of ClC-5 on NHE3 surface expression. To further understand the effects of ClC-5 on NHE3 function and distribution, we characterized the ClC-5 dependence of basal and regulated Nhe3 activity in mouse proximal tubules and then studied basal and stimulated apical distribution and rates of endocytosis and exocytosis of NHE3 in the proximal tubule-like opossum kidney (OK) cell line using short hairpin RNA (shRNA) to silence ClC-5. We show evidence that ClC-5 is necessary for NHE3 exocytosis but not endocytosis and that decreased ClC-5 lowers the amount of NHE3 on the proximal tubule apical membrane in the absence of elevated luminal PTH.

EXPERIMENTAL PROCEDURES

Mouse Models—The *Clcn5* KO mice were maintained under standard light and climate conditions in the animal facility of The Johns Hopkins University School of Medicine with *ad libitum* access to water and chow. All animal procedures were approved by the Animal Use Committee of The Johns Hopkins University. Isoflurane was used for sacrificing the mice. Single tubule perfusion experiments were approved by the Animal Use Committee of Yale University.

Materials—SNARF-4F acetoxymethyl ester, culture media, penicillin, and streptomycin were from Invitrogen. HOE694 was a gift from J. Puenter of Sonafi-Aventis (Frankfurt, Germany). Forskolin, dexamethasone, bovine PTH, and L-glutathione were from Sigma-Aldrich. A23187 was from Calbiochem (Gibbstown, NJ). EZ-Link sulfo-NHS-SS-biotin, sulfo-NHS-acetate, and immunopure avidin were from Thermo Scientific (Pierce). The rabbit polyclonal anti-Clc-5 antibody used in this study was produced and affinity-purified at Covance (Princeton, NJ) to the antigen "KSRDRDRHREITNKS" from the human ClC-5 N-terminal domain. This peptide has been used previously to generate antibodies to ClC-5 (3, 16). The mouse monoclonal anti-β-actin antibody was from Sigma-Aldrich (catalog number A5441), and the mouse monoclonal anti-GAPDH antibody was from United States Biological (Swampscott, MA; catalog number G8140-11). The 3H3 monoclonal mouse anti-opossum NHE3 antiserum was a gift from Orson Moe (University of Texas Southwestern Medical Center, Dallas, TX). The polyclonal rabbit anti-megalin antiserum was a gift from Daniel Biemesderfer (Yale University, New Haven, CT). Anti-NHERF2 rabbit polyclonal antibody was produced as described previously (24). IRDye800CW, a goat-conjugated affinity-purified anti-mouse IgG (heavy and light chains) was from Rockland Inc. (Philadelphia, PA). Horseradish peroxidase-labeled anti-mouse IgG was from Amersham Biosciences. The enhanced chemiluminescence detection kit was from PerkinElmer Life Sciences.

Isolated Kidney Cortex—Mice, as described previously (3) (studied between 8 and 12 weeks of age), were briefly anesthetized with isoflurane and then sacrificed by cervical dislocation. The abdomen was immediately opened, and the kidneys were removed and placed over ice in an ice-cold Na^+ buffer (buffer A) containing 138 mM NaCl, 5 mM KCl, 2 mM $CaCl_2$, 1 mM $MgSO_4$, 1 mM NaH_2PO_4, 25 mM glucose, 20 mM HEPES, and 1 mM probenecid, pH 7.4. The kidney was cut in half, the capsule was removed, and 1–1.5-mm slices were cut with a razor blade. These slices were mounted with Krazy Glue (Elmer's Products Inc., Columbus, OH) onto a glass coverslip (22).

Measurement of Renal Cortical NHE3 Activity by Multiphoton Microscopy/SNARF-4F—Methods used for the multiphoton experiments have been published previously (25). Briefly, renal cortical slices fixed to a glass slide with Krazy Glue were loaded with 20 μM SNARF-4F in a sodium buffer at 37 °C for 35 min. Tissue was then placed on the stage in a multiphoton microscope, perfused using a peristaltic pump with a Na^+ buffer for 15 min, and then acidified for 30 min using a 60 mM NH_4Cl prepulse followed by perfusion with tetramethylammonium (TMA) buffer for 20–25 min (containing 130 mM tetramethylammonium chloride, 5 mM KCl, 2 mM $CaCl_2$, 1 mM $MgSO_4$, 1 mM NaH_2PO_4, 25 mM glucose, and 20 mM HEPES, pH 7.4).

To monitor Na^+/H^+ exchange activity as the initial rate of pH_i recovery, the TMA buffer was quickly switched to Na^+ buffer, which was identical to TMA buffer except Na^+ replaces TMA (26). Both buffers contained 50 μM HOE694 to eliminate the contributions of NHE1 and NHE2 to the ΔpH_i. Reagents (pretreatment with 10 μM forskolin for 15 min, 2.5 μM A23187 for 45 min, and 10 μM dexamethasone for 2 h) were added to all perfusion buffers, and time of exposure refers to time before exposure to Na^+ buffer. 1 mM probenecid was in all perfusates to prevent SNARF-4F leakage. Because resulting SNARF-4F leakage in kidney was small, one slice of kidney cortex could be used for two sequential acidifications/NHE3 measurement cycles, each using an NH_4Cl prepulse. Either two controls on one slice or a control followed by a test condition was performed. In dexamethasone experiments, control and dexamethasone treatments were done on different slices. There was no pH_i recovery when Na^+ was added as above in the presence of 50 μM HOE694 when 10 μM ethylisopropylamiloride was included, demonstrating that NHE3 activity was being measured.

Analysis of Collected Images—Images for each optical section of kidney cortex, 0–50 μm from the surface at 5-μm steps (see Fig. 1, *A* and *B*), were taken at 580 and 640 nm and stored. These conditions allowed quantifiable signals to be studied at depths up to 40–50 μm from the cortical surface. Below that, the signal became too dim to obtain quantitative ratiometric data. Optical images for analysis were taken typically starting at 20 μm below the cut surface of the kidney cortex to avoid damaged cortical cells from the slice preparation. Regions of interest (ROIs), including regions for measurements of background, were randomly chosen in five to six individual proximal tubules. Fluorescence intensity in gray levels that correspond to relative

amounts of SNARF-4F for each ROI (16–21 ROIs per time point) for both 640- and 580-nm emissions was calculated using NIH ImageJ. The intensity of the background was subtracted from each chosen ROI. The 640/580 nm ratio for each ROI was calculated, average values of ROIs were determined for each time point, and 640/580 nm ratios over time were determined followed by conversion to pH values with internal pH standards using Microsoft Excel. The Na^+/H^+ exchange activity of NHE3 was determined as the initial rate in pH change by calculating the initial steep pH_i slope after the addition of Na^+ buffer using linear curve fit analysis (Origin 6.0, OriginLab Corp., Northampton, MA) and is presented as ΔpH/min.

Single Tubule Determination of HCO_3^- Absorption—Superficial proximal tubules were perfused *in vivo* by a method similar to those described previously (3, 27). WT and *Clcn5* knock-out mice were anesthetized by intraperitoneal injection of 100 mg/kg body weight Inactin (5-ethyl-5-(1-methylpropyl)-2-thiobarbituric acid) from Sigma-Aldrich and then placed on a thermostatically controlled surgical table to maintain body temperature at 37 °C. After tracheotomy, the left jugular vein was cannulated with a PE-10 catheter for intravenous infusion of normal saline solution at a rate of 0.15 ml/h. The left kidney was exposed by a lateral abdominal incision, isolated, and immobilized in a kidney cup filled with light mineral oil (37 °C). A proximal convoluted tubule with three to five loops on the kidney surface was selected and perfused using a Hampel-type microperfusion pump at a rate of 15 nl/min with a proximal oil block. Tubule fluid collections were made downstream using another micropipette with an oil block on the distal side. The perfusion solution contained 0.1% FD&C green dye for identification of the perfused loops. After fluid collections, the perfused tubules were marked with heavy mineral oil stained with Sudan black. After the experiment, the perfused tubules were filled with high viscosity Microfil (Canton Bio-Medical Products, Boulder, CO). The kidney was partially digested in 20% NaOH, then silicone rubber casts of the tubule segments were dissected, and the tubular length was measured. The rate of net HCO_3^- absorption was measured and calculated based on changes in the concentrations of total CO_2. The total CO_2 concentrations in both initial and collected fluids were measured by the microcalorimetric (picapnotherm) method (27). The rate of net HCO_3^- absorption was calculated per minute per millimeter of proximal tubule.

Construction of shRNAi Plasmids for Use in OK Cells—shRNA primers specific for knocking down ClC-5 were designed to the mouse nucleotide sequence NM_016691.2 using the Invitrogen mouse website. The constructs used were 5′-GCA GCA AGT TCC CTT CTA AAG-3′ (shRNA-c27; c27) and 5′-GCA TTT ATG ATG CCC ACA TCC-3′ (shRNA-c1869, c1869). Three other constructs, 5′-GGT GGT GGA ATA GGC TCT TCA-3′ (shRNA-c173; c173), 5′-GCT TCT GTG ATA CTG CAT TAG-3′ (shRNA-c2638; c2638), and 5′-GCT GCT GTG GGA ACA TCT TGT-3′ (shRNA-c858; c858) gave smaller amounts of silencing. Primers were cloned into the vector pENTRTM/U6 (Invitrogen) using the U6 promoter and RNA polymerase III terminator sites. In addition, a scrambled construct (sc) having the same base pair composition as shRNA-c27 (5′-GGC ACT AAC GTC CAC TAT GTA-3′) was cloned into the same vector and used as a control in all shRNAi experiments. The protein level of ClC-5 was measured by Western blotting to evaluate the effect of knockdown (KD) of ClC-5 by shRNA.

OK Cells in Culture and Transfection—Didelphis virginiana OK cells from ATCC were used for surface expression of NHE3 and megalin as well as measurement of NHE3 exocytosis and endocytosis. OK cells were cultured at 37 °C in a 95% air, 5% CO_2 atmosphere and passaged in Dulbecco's modified Eagle's medium supplemented with 10% fetal bovine serum, 100 units/ml penicillin, and 100 μg/ml streptomycin. Cells were seeded onto plastic dishes (day 1) and grown overnight to ~35% confluence, and then the shRNA expression plasmids were transfected using Lipofectamine 2000 according to the manufacturer's instructions (Invitrogen). The percentage of cells transfected was ~85–90% based on cotransfection with GFP and was optimized for the amounts of plasmid and Lipofectamine. OK cells were grown to 4 days postconfluence and then serum-starved for 1 day before the study. Experiments were performed on day 5 after transfection.

Surface Expression of NHE3 and Megalin Measured by Cell Surface Biotinylation—Measurement of surface proteins followed biotinylation methods published previously (28, 29). To measure surface NHE3, day 5 postconfluency OK cell monolayers were chilled to 4 °C by rinsing with ice-cold phosphate-buffered solution containing 0.1 mM Ca^{2+} and 1.0 mM Mg^{2+} (PBS-Ca-Mg). Cells were incubated for 30 min with gentle shaking in an alkaline borate buffer with 1.25 mg/ml NHS-SS-biotin, and this was repeated once. After rinsing with PBS-Ca-Mg, cells were washed twice for 10 min with 100 mM glycine in PBS-Ca-Mg to scavenge unreacted biotin and then scraped into lysis buffer (20 mM Tris, 150 mM NaCl, 1 mM EDTA, and 1% Triton X-100, pH 7.4) with protease inhibitors (28). Lysates were incubated with avidin-agarose beads to precipitate the biotinylated proteins. The beads were washed three times with PBS with 0.1% Triton X-100, and the biotinylated proteins were separated by SDS-PAGE and transferred to nitrocellulose membranes for quantitative Western blotting using anti-megalin and anti-NHE3 antibodies. For surface biotinylated megalin and NHE3, GAPDH was used to determine contamination of any intracellular biotin. GAPDH or actin was also used as a loading control for total NHE3 and megalin. The Odyssey system and Odyssey software (LI-COR Biosciences, Lincoln, NE) or chemiluminescence and NIH ImageJ and Microsoft Excel software were utilized to quantify surface and total amounts of NHE3 and megalin.

In separate experiments, as described previously (30), OK cells were incubated in serum-free medium with PTH (0.5 μM) or vehicle for 40 min at 37 °C. Cells were rinsed, cell surface-biotinylated at 4 °C, and quenched, and quantification of surface and total NHE3 was then performed as described above.

Rate of Endocytosis of NHE3 Stimulated by PTH—Endocytosis was measured by a protocol slightly modified from the reduced glutathione (GSH)-resistant endocytosis assay described previously by us (29). 5 days postconfluency, polarized OK cells were serum-starved for 24 h and labeled with 1.5 mg/ml sulfo-NHS-SS biotin for 30 min at 4 °C (this was repeated once), and then non-bound biotin was quenched as

above. Cells were rinsed with PBS at 37 °C and then incubated in serum-free medium with PTH (0.5 μm) at 37 °C for 0, 20, 35, or 50 min. Dishes were rinsed with ice-cold phosphate-buffered saline twice. Surface biotin was cleaved with GSH-containing buffer (150 mM GSH, 150 mM NaCl, and 50 mM Tris-HCl, pH 8.8) as above. The biotinylated NHE3 that was endocytosed was protected from cleavage by GSH. Cells were then solubilized in lysis buffer, biotinylated proteins were retrieved with streptavidin beads, and internalized NHE3 was assayed as described above via Western analysis and normalized to the surface NHE3 initially present.

Dexamethasone (DEX)-mediated Changes in Steady-state Surface Expression of NHE3—Measurement of dexamethasone-mediated changes in cell surface levels of NHE3 followed the method of Bobulescu *et al.* (31). Apical surface proteins were initially blocked with 1.5 mg/ml sulfo-NHS-acetate at 4 °C for 2 h. This blocking step acetylates all accessible surface amine groups, providing a low background against which newly appearing surface NHE3 could be measured. After quenching (100 mM glycine in PBS-Ca-Mg), cells were then switched to serum-free medium with or without DEX (1 μM) at 37 °C for 3 h. Surface proteins were then biotinylated twice for 30 min each and processed as above.

Exocytosis of NHE3 in Basal Conditions or after Stimulation by Dexamethasone—To measure exocytosis of NHE3 in basal conditions, confluent serum-starved OK cells were rinsed with PBS-Ca-Mg two times at 4 °C. Surface proteins accessible to NHS-SS-biotin were masked by reaction with membrane-impermeant NHS-acetate (1.5 mg/ml) at 4 °C for a total time of 2 h, adding fresh NHS-acetate every 40 min. Then cells were incubated with quenching buffer (100 mM glycine in PBS-Ca-Mg) twice with gentle shaking for a total time of 20 min at 4 °C. After quenching, cells were incubated with prewarmed serum-free medium for 3, 5, and 7 min at 37 °C. One set of cells treated with sulfo-NHS-acetate at 4 °C but never warmed to 37 °C served as the zero time point. Cells were then labeled with sulfo-NHS-SS-biotin (0.3 mg/ml) and treated with lysis buffer as described above. The biotinylated fraction was precipitated with avidin-agarose beads. The resultant precipitate was subjected to SDS-PAGE, and biotinylated NHE3 was detected by Western blot analysis as described above.

For measurement of exocytosis of NHE3 in response to dexamethasone, confluent serum-starved OK cells were treated with or without dexamethasone (1.5 μM) for 2.5 h at 37 °C. Then cells were treated with NHS-acetate, washed with quenching buffer as above, and then incubated with prewarmed serum-free medium for 4 min at 37 °C. The accessible surface membrane proteins were labeled with biotin, the biotinylated fraction was precipitated with avidin-agarose beads, and the surface biotinylated NHE3 was detected by Western blot analysis.

Statistics—The data for NHE3 activity in the kidney cortex were analyzed with Origin 8.0 software (OriginLab Corp.). In all experiments, p values were determined using Student's unpaired or paired t tests as indicated. Values are presented as the mean ± S.E.

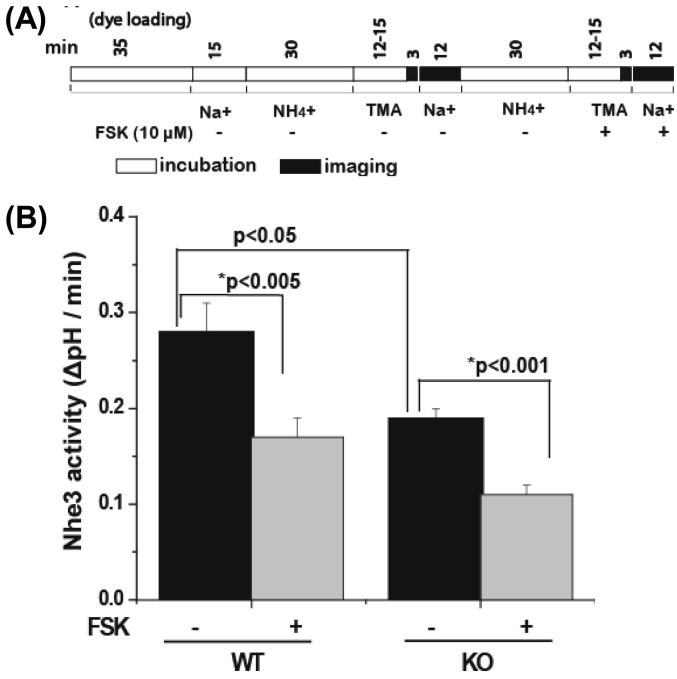

FIGURE 1. **Basal NHE3 activity is reduced in proximal tubules of kidney cortex from *Clcn5* KO mice compared with WT, but forskolin causes similar percent inhibition of NHE3 activity in both.** *A*, the time line of the experiments performed on the kidney cortex. Kidney cortex slices from WT and *Clcn5* KO mice were loaded with 20 μM SNARF-4F for 35 min at 37 °C in Na^+ buffer before NH_4Cl exposure. NH_4Cl, TMA, and Na^+ buffers had 50 μM HOE694 added to inhibit NHE1 and NHE2 activity. Forskolin (*FSK*) (10 μM) was perfused over the tissue for ~15 min before Na^+ addition. *B*, NHE3 activity is presented as the initial rates (ΔpH/min). Results are expressed as the mean ± S.E. of experiments for WT ($n = 6$) and *Clcn5* KO ($n = 6$). **p* values are a comparison of basal and forskolin-treated kidney proximal tubules (paired t test), and p values are a comparison of basal NHE3 activity of WT and *Clcn5* KO (unpaired t test).

RESULTS

Loss of ClC-5 Reduces Basal Nhe3 Activity in Murine Proximal Tubules—Basal Nhe3 activity (ΔpH/min) was determined under conditions in which Nhe2 and Nhe1 were inhibited by 50 μM HOE694. As shown in Fig. 1 and Table 1, Nhe3 activity was reduced by 26 ± 10% ($n = 17$, $p < 0.0001$) in *Clcn5* KO (0.20 ΔpH/min ± 0.02, $n = 17$) compared with WT (0.29 ΔpH/min ± 0.04, $n = 17$).

Second Messenger Inhibition of Nhe3 Activity Is Not Changed in Clcn5 KO Proximal Tubules, but Stimulation by Dexamethasone Is Reduced—To determine whether acute inhibition of Nhe3 was altered in *Clcn5* KO proximal tubules, permeable second messengers were used to eliminate possible changes related to ClC-5 in signaling molecules at steps between ligand binding and second messenger generation. The effects of forskolin (10 μM) or A23187 (2.5 μM) on Nhe3 activity were determined. The initial rate of Nhe3 activity (ΔpH/min) in WT mouse proximal tubules treated with forskolin (10 μM) was decreased by 40 ± 6% ($p < 0.001$) (Fig. 2 and Table 1). In *Clcn5* KO proximal tubules, forskolin also reduced Nhe3 activity by 41 ± 5% ($p < 0.001$) (Fig. 1 and Table 1), an effect similar to that in WT. In another series of experiments, the initial rate of Nhe3 activity in WT proximal tubules was reduced by 38 ± 5% after A23187 treatment and reduced by 36 ± 8% in *Clcn5* KO proximal tubules (Fig. 2 and Table 1), suggesting a similar effect of A23187 on Nhe3 activity in WT and *Clcn5* KO.

TABLE 1
Initial rates of NHE3 activity in intact mouse proximal tubules (ΔpH/min)
↓, reduced; ↑, increased.

	WT					KO				
	n	Untreated	Treated	Change	*p*	*n*	Untreated	Treated	Change	*p*
		ΔpH/min	*ΔpH/min*	*%*			*ΔpH/min*	*ΔpH/min*	*%*	
Forskolin (10 μM)	6	0.27 ± 0.03	0.16 ± 0.01	↓ 40 ± 6	<0.01[a]	6	0.19 ± 0.01	0.11 ± 0.01	↓ 41 ± 5	<0.001[a]
A23187 (2.5 μM)	6	0.30 ± 0.04	0.19 ± 0.02	↓ 38 ± 5	<0.005[a]	6	0.21 ± 0.02	0.13 ± 0.01	↓ 36 ± 8	<0.01[a]
DEX (10 μM)	5	0.29 ± 0.02	0.40 ± 0.03	↑ 40 ± 7[b]	<0.005	5	0.21 ± 0.01	0.24 ± 0.01	↑ 14 ± 5[b]	<0.05
Basal activity	17	0.29 ± 0.04				17	0.20 ± 0.02			<0.0001

[a] Determined using Student's paired *t* test.
[b] Comparing percent increase in NHE3 activity caused by dexamethasone treatment, WT *versus Clcn5* KO, $p < 0.01$.

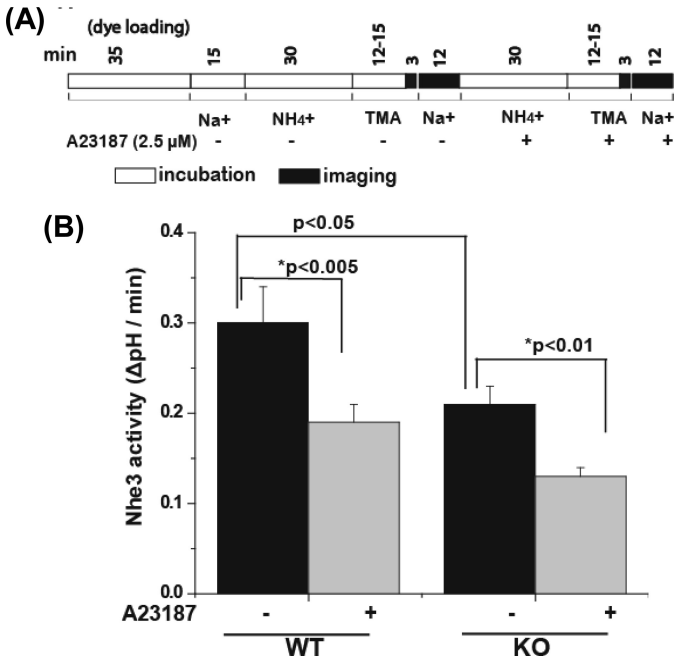

FIGURE 2. **Ca^{2+} ionophore A23187 causes similar percent inhibition of NHE3 activity in kidney cortex from WT and *Clcn5* KO mice.** *A*, the time line of the experiments performed on the kidney cortex using the same conditions as in Fig. 1 except for the use of 2.5 μM A23187 to increase intracellular calcium. *B*, NHE3 activity was measured by the initial rate of alkalinization (ΔpH/min). Results are expressed as means ± S.E. of experiments for WT ($n = 6$) and *Clcn5* KO ($n = 6$). *p* values were calculated as described in Fig. 1.

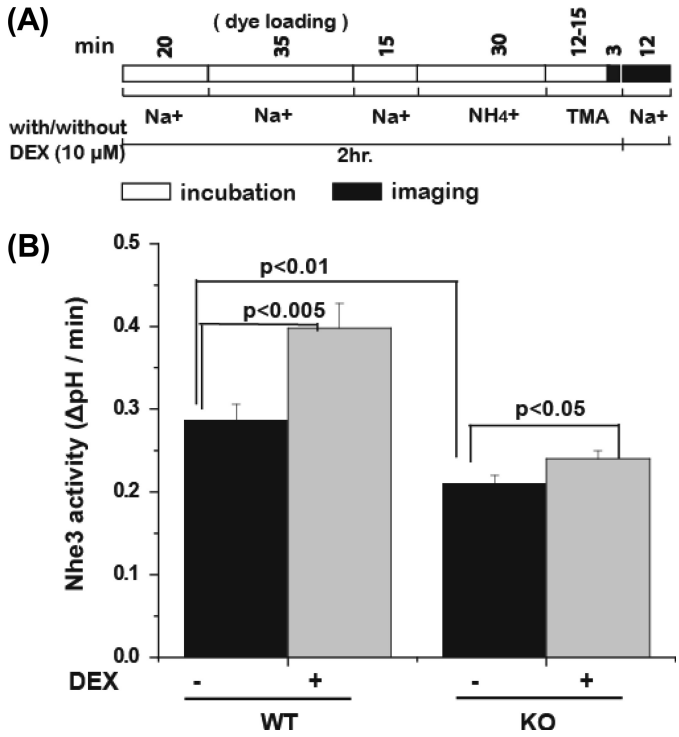

FIGURE 3. **DEX (2-h) stimulation of NHE3 activity is less in kidney cortex of *Clcn5* KO mice compared with WT.** *A*, the time line of the experiments performed on the kidney cortex using conditions shown in Fig. 1. The incubation with 10 μM DEX occurred over a 2-h period, including during the dye loading period, during the initial perfusion stage, and when Na^+ was absent. *B*, NHE3 activity is reported as an initial rate (ΔpH/min). Results are expressed as means ± S.E. of five experiments for WT and six experiments for *Clcn5* KO. *p* values are a comparison of wild-type and *Clcn5* KO NHE3 activity with no DEX treatment (basal NHE3 activity) (*black bars*) or a comparison of no DEX and DEX treatment for WT and *Clcn5*-null slices.

DEX (10 μM; 2 h) pretreatment was used as a model of acute stimulation of Nhe3 activity, a time before changes in transcription increased changes in Nhe3 protein expression (31). DEX stimulated Nhe3 activity in WT mouse proximal tubules by 40 ± 7% over basal activity ($p < 0.005$) (Fig. 3 and Table 1), whereas in the *Clcn5* KO mouse, the increase was significantly less ($p < 0.01$), being only 17 ± 5% ($p < 0.05$) (Fig. 3 and Table 1). The DEX effect was reduced by 23 ± 3% in *Clcn5* KO mice compared with WT mice. Overall these experiments show that 1) basal Nhe3 activity is decreased in the *Clcn5* KO mice compared with WT, 2) DEX stimulation of Nhe3 activity is reduced in the *Clcn5* KO mice, and 3) inhibition of Nhe3 activity by forskolin and A23187 does not depend on ClC-5 in the renal proximal tubule.

Transepithelial Bicarbonate Movement Is Reduced in Clcn5 KO—In situ single tubule perfusion was used to measure WT and *Clcn5* KO mouse proximal tubule transepithelial bicarbonate movement, a process that is due to Nhe3 activity (Table 2). The bicarbonate flux in WT proximal tubules was 109.9 ± 7.3 pmol/min/mm of tubule length. In *Clcn5* KO tubules, this flux was 77.4 ± 10.1 pmol/min/mm of tubule length, a 30% decrease ($p < 0.05$). This decrease in transepithelial movement of bicarbonate absorption is sim-

TABLE 2
Bicarbonate absorption in kidney proximal tubules of WT and Clcn5 KO mice
Data are mean ± S.E. *N*, number of perfused tubules; *n*, number of animals; V_o, perfusion rate; *L*, tubular length; $[HCO_3]_o$, bicarbonate concentration in the original perfusate; $[HCO_3]_L$, bicarbonate concentration in collected fluid; J_{HCO_3}, bicarbonate absorption.

	N/n	V_o	*L*	$[HCO_3]_o$	$[HCO_3]_L$	J_{HCO_3}
		nl/min	*mm*	*mM*	*mM*	*pmol/min/mm*
WT	13/4	15.0 ± 0.1	1.54 ± 0.2	25.26 ± 0.1	17.65 ± 1.0	109.9 ± 7.3
KO	11/4	15.1 ± 0.1	1.63 ± 0.3	25.1 ± 0.01	20.35 ± 1.3[a]	77.4 ± 10.1[a]

[a] Significant difference from control ($p < 0.05$).

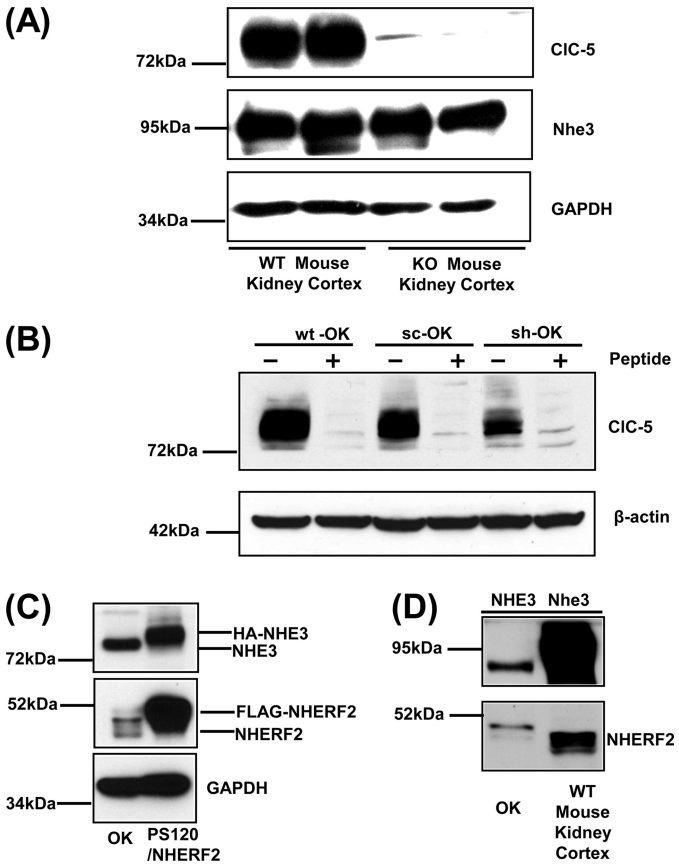

FIGURE 4. **Anti-ClC-5 antibody recognizes a protein in wild-type mouse proximal tubule and OK cells.** *A*, equal amounts of protein (40 μg) from mouse cortical lysates (WT and *Clcn5* KO mice) were applied to each lane and subjected to 10% SDS-PAGE. The protein levels of ClC-5, NHE3, and GAPDH were detected by corresponding antibodies. One representative blot is shown from three independent experiments. *B*, ClC-5 protein was detected in cell lysates from OK cells transfected with sc or sh and OK cells without transfection (WT) by Western blot analysis. Equal amounts of protein (40 μg) from sc, sh, and WT groups were applied to each lane and subjected to 10% SDS-PAGE. Proteins were transferred to nitrocellulose membrane. A peptide displacement assay was performed in sc, sh, and WT groups. For the peptide minus group, ClC-5 antibody was preincubated without peptide on ice for 30 min. For peptide plus groups, ClC-5 antibody was preincubated with peptide (100 μg/ml) on ice for 30 min. One representative blot is shown from three independent experiments. *C* and *D*, equal amounts of protein (30 μg) from lysates of OK cells, PS120 cells stably expressing FLAG-NHERF2 (*C*) (33), or kidney cortex (*D*) were applied to each lane and subjected to 10% SDS-PAGE. The protein levels of NHE3, NHERF2, and GAPDH were detected by corresponding antibodies. Representative blots are shown from three independent experiments.

ilar to the 31% decrease in Nhe3 activity in *Clcn5* KO compared with WT proximal tubules (see Table 1).

Standardization of OK Model of Reduced ClC-5 Using shRNA—The mechanism(s) underlying decreased basal and dexamethasone-stimulated Nhe3 activity in proximal tubules of *Clcn5* KO mice was studied using the polarized renal proximal tubule OK cell line in which shRNA was used to knockdown ClC-5 (Fig. 4). Fig. 4, *A* and *B*, show specificity of the anti-ClC-5 antibody used to quantify the efficiency of knockdown. The ClC-5 antibody recognized a band of ~80 kDa in kidney cortex of WT mouse. No signal of ClC-5 was detectable in *Clcn5* KO. The protein level of NHE3 in *Clcn5* KO mouse had no change compared with that in WT mouse, suggesting that decreased Nhe3 activity in *Clcn5* KO mouse is not due to alterations of total Nhe3 protein (Fig. 4*A*). As shown in Fig. 4*B*, an ~80-kDa protein band was identified in cell lysates from OK cells transfected with sc or shRNA-c27 (sh) and WT cells without transfection, although the signal of the band was reduced by the ClC-5 shRNA. Competing peptide displacement eliminated the entire signal except for minimal amounts of two bands of a size similar to ClC-5, which are interpreted as nonspecific bands. Based on previous reports (32, 33), NHERF2 is necessary for DEX stimulation of NHE3. In this study, DEX-induced exocytosis of NHE3 served as a model for elucidating the role of ClC-5 in NHE3 trafficking, although it has been reported that endogenous NHERF2 is not detected in some OK cell lines (33). Using PS120/FLAG-NHERF2 cells as a positive control for the protein level of NHERF2 (Fig. 4*C*), the OK cells used in this study do express endogenous NHERF2. The amount of endogenous NHERF2 in OK cells compared with that in mouse kidney cortex also confirmed the expression of NHERF2 protein in OK cells, although mouse kidney cortex also had higher levels of NHERF2 compared with these OK cells (Fig. 4*D*).

To create a model of ClC-5 deficiency in OK cells, shRNA was used. shRNA or scrambled constructs were transfected into OK cells and evaluated ~5 days later (supplemental Fig. 1). Transfection efficiency was 85–90% using cotransfected GFP as a marker. Two shRNA constructs lowered the level of ClC-5 by ~60%. One, c27, lowered the ClC-5 protein by 65 ± 7% (n = 32). A second construct, c1869, resulted in a decrease of 60 ± 8% (n = 7). Three other constructs caused a much smaller but significant reduction in ClC-5 expression (supplemental Fig. 1B). A scrambled construct made with the same base pairs as c27 did not alter the expression of ClC-5 compared with cells without transfection with any construct (Fig. 4*B*). No construct altered expression of actin or GAPDH. One construct, c1869, also decreased NHE3 expression and was not further studied (supplemental Fig. 1C). Among all the ClC-5-silencing constructs, c27 had the greatest effect on reduction of ClC-5 expression and had no effect on NHE3 expression compared with that of the sc. Further *in vitro* studies in OK cell lines were primarily carried out with c27.

shRNA KD of ClC-5 in OK Cells Mimics Changes in Surface and Total NHE3 and Megalin Expression Seen in Clcn5 KO Mouse Renal Proximal Tubules—Surface expression of NHE3 and megalin was determined in WT and ClC-5 KD OK cells. ClC-5 was silenced by 65 ± 5% (n = 4) in these experiments using the c27 construct. As shown in Fig. 5, *A* and *B*, KD of ClC-5 significantly reduced the percentage of surface megalin and NHE3 as determined by cell surface biotinylation. In ClC-5 KD OK cells, the percentage of NHE3 on the apical surface was decreased by 39 ± 9% (n = 4, p = 0.05) compared with that in the scrambled group. Total NHE3 did not change between scrambled and KD groups (Fig. 5, *A* and *C*). As shown in Fig. 5, *A* and *C*, total megalin was also reduced in ClC-5 KD OK cells, which is similar to what was found in proximal tubules of the *Clcn5* KO mouse. These results agree qualitatively with those in *Clcn5* KO mouse proximal tubules described above and indicate that the OK cells transfected with ClC-5 shRNA plasmids are an appropriate in *vitro* model to study mechanisms by which the NHE3 surface amount depends on ClC-5 expression.

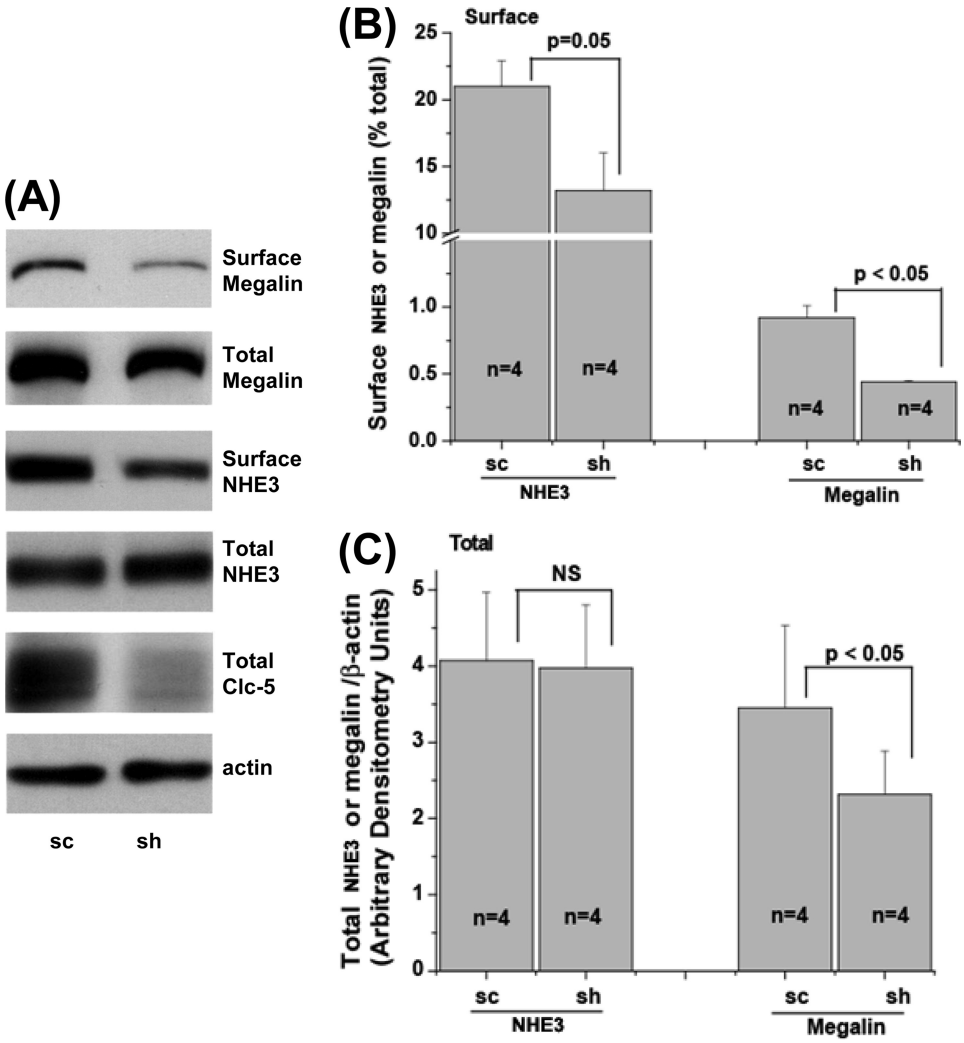

FIGURE 5. **ClC-5 KD reduces surface expression of NHE3 and megalin and total megalin in OK cells.** *A*, total and surface NHE3 and megalin of OK cells transfected with sc or sh were determined by a surface biotinylation assay as described under "Experimental Procedures." Representative blots are shown from four independent experiments. *B*, quantitative analysis of surface NHE3 or megalin by densitometry from experiments described in *A* is shown. The amounts of surface NHE3 and megalin were calculated as the percentage of total NHE3 and megalin, respectively. Results are mean ± S.E. of data from four independent experiments. *p* values are in comparison with the sc group (paired *t* test). *C*, quantitative analysis of total NHE3 or megalin by densitometry from experiments described in *A*. Total NHE3 and megalin were normalized to β-actin. Results are mean ± S.E. of data from four independent experiments. *p* values are in comparison with the sc group (paired *t* test). *NS*, not significant.

PTH-mediated Decrease in Surface NHE3 Is Not Significantly Changed by Reduction of ClC-5—The explanation for similar reductions in tubular NHE3 activity after treatment with cAMP or elevated calcium was investigated by measuring changes in surface NHE3 in OK cells using c27 to knock down ClC-5 and PTH treatment (a previously established model of stimulated proximal tubule endocytosis (30, 34)). These ClC-5 KD cells had a 63 ± 11% reduction of total ClC-5 ($n = 8$). Surface NHE3 was measured under four conditions, including sc control ± PTH and ClC-5 KD ± PTH. All results were normalized to total NHE3/GAPDH, which was not different under any of these conditions (see Fig. 6, *A* and *C*). The surface NHE3/total NHE3 after a 40-min PTH incubation in the sc-treated cells was set at 100% in each experiment ($n = 4$). In the absence of PTH, surface NHE3 in ClC-5 KD cells was reduced by 29 ± 5% compared with that in sc-treated cells ($p < 0.05$, $n = 4$). In sc-treated cells, PTH reduced surface NHE3 by 41 ± 8% ($p < 0.05$, $n = 4$). In ClC-5 KD cells, PTH reduced surface NHE3 by 29 ± 9% ($p < 0.05$, $n = 4$). The relative reduction of surface NHE3 caused by PTH in ClC-5-silenced and scrambled construct cells was not significantly different ($p = 0.16$).

PTH-stimulated Rate of Endocytosis of NHE3 Is Not Different in OK Cells Transfected with sc and sh—Because Clcn-5 KO mice have demonstrated reduced rates of endocytosis in some conditions, PTH-stimulated endocytosis of NHE3 was measured in sc and ClC-5 KD OK cells (Fig. 7) . The amount of NHE3 internalized at 20, 35, and 50 min was normalized to the surface NHE3 that was at 4 °C and was not treated with GSH (Control). The rate of NHE3 endocytosis in ClC-5 sc cells treated with PTH was 0.78 ± 0.04% of initial surface NHE3 internalized per minute ($n = 3$), and the rate in sh c27 cells was 0.68 ± 0.05% of initial surface NHE3 internalized per minute ($n = 3$). ClC-5 was silenced by 66 ± 7% ($n = 3$). Taken together, the rate of NHE3 endocytosis was not significantly different between the sc group and sh group, showing that PTH-related endocytosis was not altered by ClC-5 KD in OK cells.

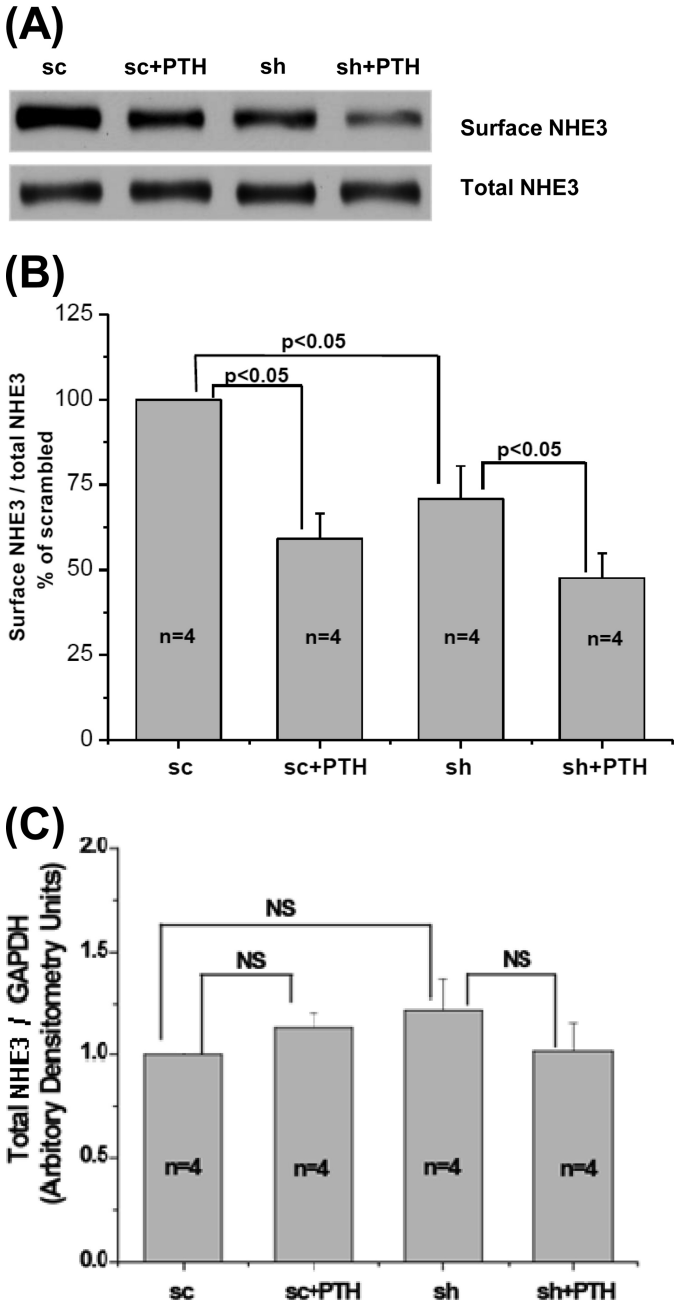

FIGURE 6. **Endocytosis of NHE3 stimulated by 0.5 μM PTH (40 min) is not different between scrambled OK cells and cells with ClC-5 KD.** OK cells transfected with sc or sh construct were incubated with or without PTH (0.5 μM) for 40 min at 37 °C. Surface NHE3 was determined as described under "Experimental Procedures." *A*, a representative blot from four independent experiments is shown. *B*, quantitative analysis of surface NHE3 by densitometry from experiments described in *A*. Values of surface NHE3/total NHE3 were calculated as the percentage of untreated sc group. Results are mean ± S.E. of data from four independent experiments. *p* values are in comparison with the corresponding untreated sc group or sh group (paired *t* test). *C*, quantitative analysis of total NHE3 by densitometry from experiments described in *A*. Total NHE3 was normalized to GAPDH, and values of total NHE3/GAPDH were calculated as the percentage of untreated sc group. Results are mean ± S.E. of data from four experiments. *p* values are in comparison with the corresponding untreated sc group or sh group (paired *t* test). *NS*, not significant.

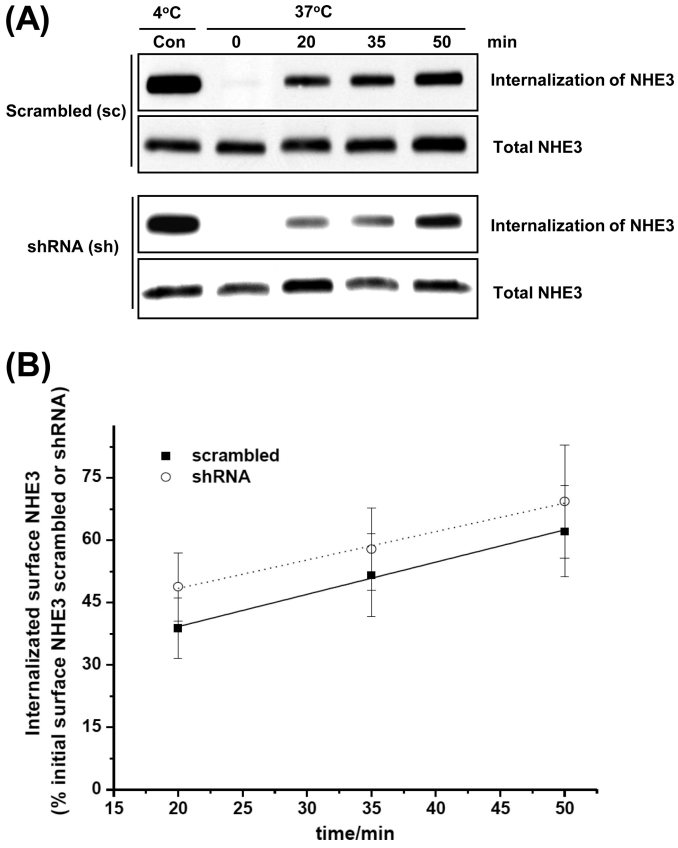

FIGURE 7. **Rate of endocytosis of NHE3 in response to PTH is not significantly different between scrambled and ClC-5 silenced cells.** OK cells transfected with sc or sh constructs were incubated at 37 °C in the presence of PTH (0.5 μM) for 0, 20, 35, and 50 min. The amount of endocytosis of NHE3 (internalization of surface NHE3) at the above indicated time points was determined by a GSH-resistant endocytosis assay as described under "Experimental Procedures." *A*, a representative blot from three independent experiments is shown. *B*, quantitative analysis of endocytosis of NHE3 by densitometry from experiments described in *A*. The amount of internalized NHE3 via endocytosis at each time point (20, 35, and 50 min) was calculated as the percentage of surface NHE3 of the corresponding control group, which was always kept at 4 °C and was not exposed to GSH. The slopes of endocytosis of NHE3 were calculated to determine the rates of endocytosis in sc and sh groups as shown in *A*. Results are mean ± S.E. of data from three independent experiments. *Con*, control.

DEX-mediated Increased Steady-state Amount of NHE3 Is Reduced in ClC-5 KD OK Cells—An important difference between WT and *Clcn5* KO mouse proximal tubules was the failure of *Clcn5* KO tubules to significantly increase NHE3 activity after 3 h of DEX exposure. Because DEX has been shown to increase exocytosis of NHE3 in PS120 fibroblasts and OK cells (31, 33), the effect of ClC-5 KD was determined on basal and DEX-stimulated surface amounts of NHE3 over 3 h (thus measuring the steady-state levels of surface NHE3) (Fig. 8). As shown in Fig. 8, *A* and *B*, 1 μM DEX treatment for 3 h increased the steady-state surface levels of NHE3 compared with untreated control with no change in the total amount of NHE3 (Fig. 8, *A* and *B*). The reduction of total ClC-5 by shRNA silencing was 66 ± 3% ($n = 4$) in untreated cells and 58 ± 4% ($n = 4$) in cells treated with DEX. In response to DEX, the percentage of NHE3 on the apical surface of scrambled OK cells was increased by 54 ± 10% ($n = 4$, $p < 0.005$). In contrast, in the ClC-5 KD OK cells, the DEX-mediated increase in the percentage of NHE3 on the apical surface did not reach statistical significance (20 ± 8%, $n = 4$, not significant). Of note was the reduced surface NHE3 at 3 h in untreated ClC-5 KD compared with untreated scrambled OK cells. Again, there was no change

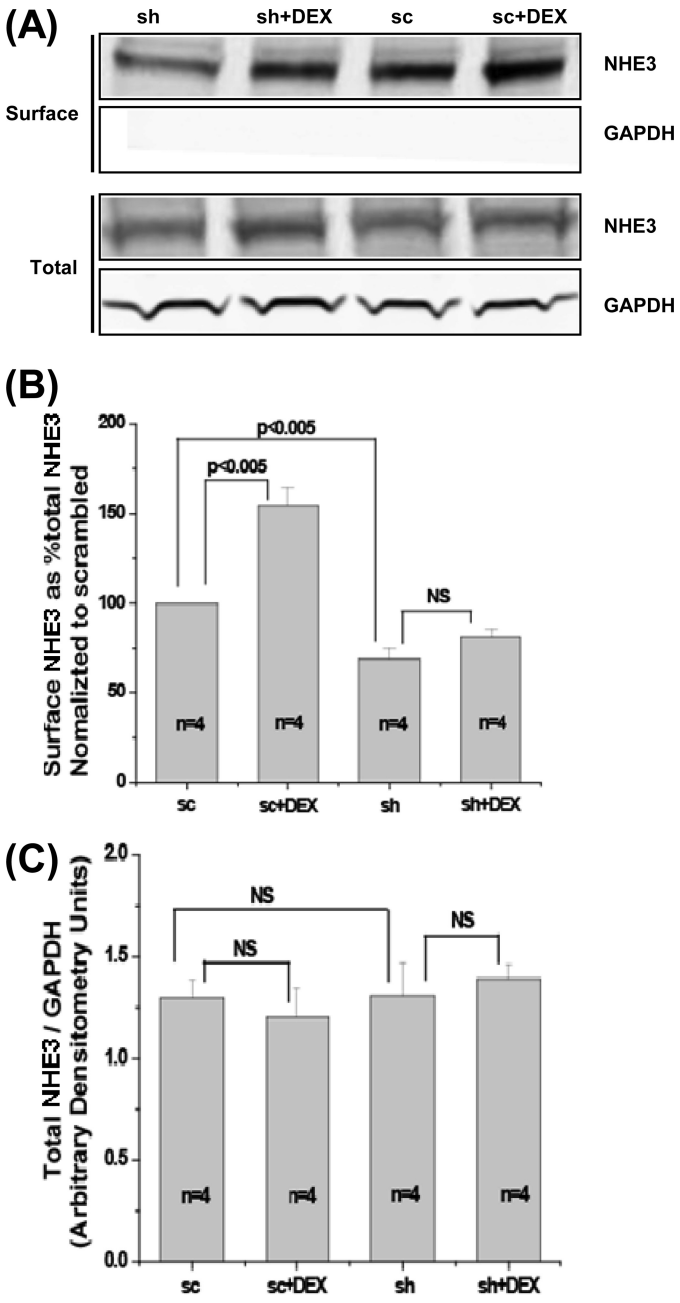

FIGURE 8. **Surface NHE3 in OK cells is significantly increased by 1 μM DEX (3-h treatment) in scrambled OK cells but not when ClC-5 is silenced in steady-state studies.** *A*, OK cells transfected with sc or sh construct were blocked with NHS-acetate twice for a total of 60 min at 4 °C. Cells were then washed and incubated at 37 °C in serum-free medium with or without 1 μM DEX treatment for 3 h. Then surface NHE3 and total NHE3 were determined by a surface biotinylation assay described under "Experimental Procedures." A representative blot from four independent experiments is shown. *B*, quantitative analysis of surface NHE3 by densitometry from experiments described in *A*. Values of surface/total NHE3 were calculated as the percentage of untreated sc group. Results are mean ± S.E. of data from four independent experiments. *p* values are in comparison with the corresponding untreated sc group or sh group (paired *t* test). *C*, quantitative analysis of total NHE3 by densitometry from experiments described in *A*. Total NHE3 was normalized to GAPDH, and values of total NHE3/GAPDH were calculated as the percentage of untreated sc group. Results are mean ± S.E. of data from four experiments. *p* values are in comparison with the corresponding untreated sc group or sh group (paired *t* test). *NS*, not significant.

in the total NHE3 amount in ClC-5 KD cells. Taken together, these data indicate that the degree of increase of surface NHE3 caused by DEX with ClC-5 silenced was significantly lower than that seen in scrambled cells. The similarity of results in *vitro* and in the *Clcn5* KO mouse proximal tubules in *vivo* is another indication that the OK model can be used to understand how ClC-5 regulates NHE3 activity and its distribution and suggests a possible role for ClC-5 in basal and dexamethasone stimulation of NHE3 exocytosis.

ClC-5 KD Reduced Basal and Prevents DEX-stimulated Exocytosis of NHE3 in OK Cells—Rates of NHE3 exocytosis were determined in OK cells expressing scrambled and ClC-5 KD shRNA. NHE3 exocytosis was linear between 0 and 7 min (Fig. 9, *A* and *B*). As shown in Fig. 9*C*, the basal initial rate of exocytosis was reduced in the ClC-5 KD cells by 47% compared with that of scrambled cells ($n = 3$, $p < 0.005$). Further studies were performed during the period of linear exocytosis (4 min). To confirm that DEX treatment stimulated exocytosis in this model, exposure of OK cells to 1.5 μM DEX for 2.5 h was used to further reduce the possible contribution to an increase in the amount of NHE3 via DEX-stimulated transcription of NHE3. As shown in Fig. 9*D*, this treatment with DEX did not alter the amount of NHE3 in either the sc or sh samples. DEX increased NHE3 exocytosis in scrambled construct-treated cells by 34% ($p < 0.05$, $n = 10$; Fig. 9, *E* and *F*). In contrast, in the ClC-5 KD cells, NHE3 exocytosis was reduced in control conditions by 44% ($p < 0.05$, $n = 10$) compared with that in sc cells, and there was no increase in NHE3 exocytosis induced by DEX. These results demonstrate a role for ClC-5 in both basal and DEX-stimulated exocytosis of NHE3.

DISCUSSION

Several striking abnormalities have been documented in the proximal tubule of the *Clcn5* KO mice. In the face of normal gross structure in the young mice studied (4), there are markedly reduced apical amounts of Nhe3, Npt2a, and megalin along with reduced total Npt2a and megalin (2). Although the increased urinary loss of sodium and phosphate is explained by the reduced apical expression of Nhe3 and Npt2a, the major proteins involved in the bulk of Na^+ and phosphate absorption from the kidney, the mechanisms underlying the abnormal apical distribution and consequently the reduced function of the transporters have not been determined.

We used two epithelial models to determine the consequences in renal proximal tubule of either absent or greatly reduced expression of ClC-5 on the activity of a transport protein, NHE3, which cycles between the endosomal system and the brush border under basal conditions and is acutely regulated primarily by changes in the rates of its endocytosis and/or exocytosis (35). Both in native murine proximal tubule and in a non-malignant proximal tubule cell line (OK cells), our results showed that ClC-5 was necessary to maintain basal NHE3 activity as well as for stimulation of NHE3 by short time exposure to DEX, whereas ClC-5 was not necessary for acute cAMP, elevated Ca^{2+}, and PTH inhibition of NHE3. These changes in transport were all due to abnormal trafficking of NHE3 when examined in polarized OK cells with reduced NHE3 surface expression under basal conditions due to reduced exocytosis

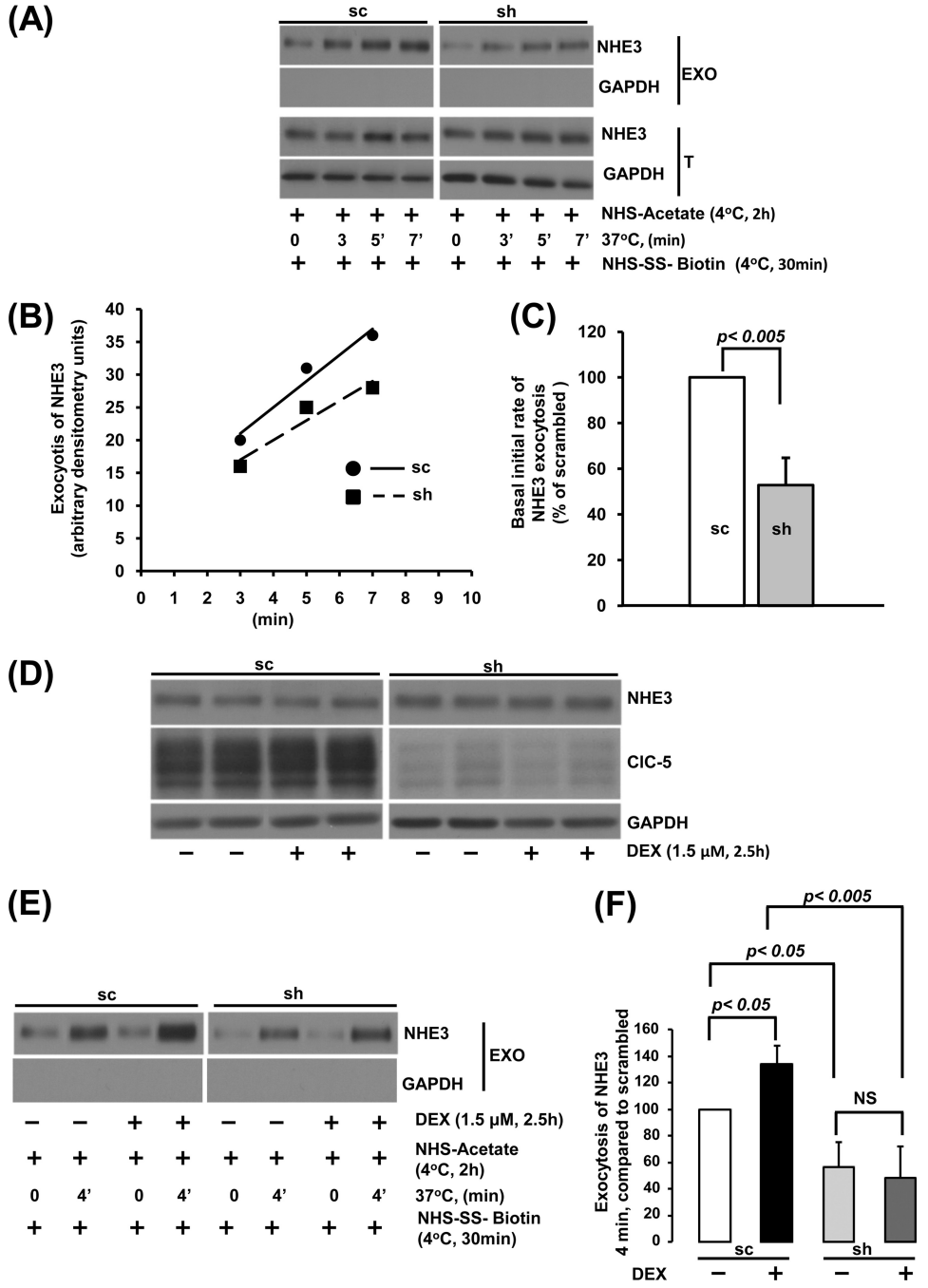

FIGURE 9. **ClC-5 knockdown decreases basal and DEX-induced exocytosis of NHE3 in OK cells.** *A*, confluent serum-starved OK cells were incubated with NHS-acetate. The *first lane* in sc and sh groups is 0 min at 37 °C. OK cells transfected with sc or sh constructs were then incubated for 3 (*second lane*), 5 (*third lane*), and 7 min (*fourth lane*) at 37 °C to allow exocytosis of NHE3. OK cells were then chilled to 4 °C, and newly inserted NHE3 (exocytosis of NHE3) was biotinylated and detected by Western blotting. GAPDH levels were measured in the surface biotinylated fraction as a negative control to ensure the absence of intracellular protein biotinylation. A representative blot from three independent experiments showed exocytosis of NHE3 under basal conditions. *B*, the surface amount of NHE3 exocytosed in *A* was measured by densitometry with signal at 0 min (background) subtracted from all time points. Arbitrary densitometry units at each time point (3, 5, and 7 min) are shown. *C*, quantitative analysis of exocytosis of NHE3 by densitometry from experiments described in *A*. The slopes of exocytosis of NHE3 within 7 min were calculated from each experiment with results of the sc group set as 100%. The basal initial rate of NHE3 exocytosis in the sh group was calculated as the percentage of that in the sc group. Results are mean ± S.E. of data from three independent experiments. *p* values are in comparison with the sc group (paired *t* test). *D*, OK cells (sc and sh) were treated with and without DEX (1.5 μM) for 2.5 h. Equal amounts of proteins (20 μg) from total lysates of cells were separated by 10% SDS-PAGE, and the levels of NHE3, ClC-5, and GAPDH were detected by Western blot analysis. A representative blot from three independent experiments is shown. *E*, OK cells were treated with and without DEX (1.5 μM; 2.5 h), exposed to NHS-acetate, and then warmed to 37 °C for 0 or 4 min. Cells were then cooled to 4 °C, and newly inserted NHE3 was detected by biotinylation and Western blotting. Intracellular GAPDH was measured in the surface-biotinylated fraction to ensure the absence of detection of intracellular proteins. A representative blot from 10 independent experiments is shown. *F*, quantitative analysis of exocytosis of NHE3 by densitometry from experiments described in *E* is shown. The value from the difference between 0 min (background) and 4 min is considered the amount of exocytosed NHE3. The amount of exocytosed NHE3 was calculated as the percentage of sc group in the absence of DEX treatment. Results are mean ± S.E. of data from 10 independent experiments. *p* values are in comparison with the corresponding untreated sc group, untreated sh group, or treated sc group (paired *t* test). *EXO*, exocytosis; *T*, total; *NS*, not significant.

and a similarly reduced DEX stimulation due to failure of DEX to stimulate exocytosis of NHE3 in the absence of ClC-5. In contrast to a role for ClC-5 in basal and stimulated exocytosis, both cAMP and elevated Ca^{2+}, both of which inhibit NHE3 at least in part by stimulating its endocytosis, caused normal percent inhibition of NHE3 in ClC-5-null mouse proximal tubule. Also PTH, which affects NHE3 by elevating both Ca^{2+} and cAMP in proximal tubule, caused a similar rate of endocytosis of NHE3 in WT and OK cells in which ClC-5 was knocked down. Moreover, given the prolonged half-life of NHE3 of ~14 h (36), the changes described here, which occurred over much shorter times, indicate that changes in brush border (BB) NHE3 were not related to changes in plasma membrane delivery of newly synthesized NHE3. We conclude that ClC-5 is necessary for basal and DEX-stimulated exocytosis but not for endocytosis of NHE3 in these epithelial cells.

This is the first detailed examination in renal proximal tubule of the dependence on ClC-5 of trafficking of Nhe3 and examination of effects on exocytosis, although the initial study of the renal phenotype of *Clcn5* KO mice identified a role for ClC-5 in proximal tubule trafficking (2). There were multiple reasons for attention to be paid first to potential effects of ClC-5 on endocytosis. *Clcn5* KO mouse renal cortex exhibited a reduced BB amount of the receptor protein megalin along with reduced total expression of megalin; megalin is the major renal proximal tubule BB receptor for endocytosis (2, 23). Also, the clinical manifestations of Dent disease are consistent with reduced proximal tubule endocytosis; there is reduced renal absorption of glucose, amino acids, and low molecular weight proteins, accounting for the glucosuria, aminoaciduria, and low molecular weight proteinuria that are part of this syndrome (5). Moreover, knocking out ClC-5 reduced proximal tubule receptor-mediated endocytosis (β_2-microglobulin and albumin) and fluid phase endocytosis (dextran and horseradish peroxidase) (37). Lastly, because NaPi2a is regulated only by endocytosis and does not undergo exocytosis, it was logical that emphasis would be on the role of ClC-5 in its endocytosis (2).

However, it was also recognized that reduced endocytosis would increase, not decrease, BB NHE3 and NaPi2a; this is the opposite of what was observed (2). Thus, it was suggested that this aspect of the pathophysiology of the lack of ClC-5 in KO mice kidney is caused by reduced PTH endocytosis/increased luminal PTH because this process is dependent on surface megalin. Thus, reduced surface NHE3 and NaPi2a were considered secondary to reduced PTH endocytosis (2). However, there were inconsistencies in the data supporting this hypothesis. For instance, other animal models in which megalin (38) and its chaperone receptor-associated protein (39) were knocked out had unaltered surface expression of NHE3. These contradictory results led us to speculate that, besides the low surface expression of megalin and consequently high concentration of tubular PTH, additional mechanism(s) might contribute to the reduced NHE3 surface expression observed in the animal model lacking ClC-5.

Recent studies focusing on molecular mechanisms of ClC-5 actions indicated that ClC-5 might have a direct role in regulation of NHE3 trafficking. Drugs that abrogate vacuolar acidification (as occurs with ClC-5 KO) did not affect the rate of endocytic uptake but inhibited recycling or transfer to lysosomes (40). In addition, ClC-5 directly interacts with NHERF2, a PDZ domain-containing protein that is essential for both endocytosis and exocytosis of NHE3 (32, 35, 41). Moreover, NHE3 has a function similar to that of ClC-5 in respect to acidification of some endosomes (37). Finally, in proximal tubules and intercalated ducts in several patients with Dent disease, the H^+-ATPase appeared on the basolateral membrane rather than in the normal BB location (42). This appears to be an example of altered polarity of a specific protein, whereas the polar distribution of multiple other proteins was normal (42). These observations suggested that ClC-5, NHE3, and H^+-ATPase might localize (at least partially) in a common compartment, and ClC-5 might regulate NHE3 trafficking. This evidence led us to examine in detail the role of ClC-5 in the trafficking of NHE3. Our data showed that under basal conditions (which is in the absence of high luminal PTH) surface expression of NHE3 is decreased in OK cells with reduced expression of ClC-5, which is similar to what is seen with megalin, suggesting that it is likely that ClC-5 plays a similar role in the regulation of trafficking of NHE3 and megalin. Furthermore, our direct measurements of NHE3 exocytosis and endocytosis demonstrate that, at least in OK cells, it was exocytosis and not endocytosis of NHE3 that depended on ClC-5.

The similarity of the ClC-5 dependence of NHE3 trafficking in intact mouse proximal tubules and OK cells is surprising because it has been suggested that in proximal tubules NHE3 inhibition by trafficking from the microvilli is primarily to a domain just superior to the intermicrovillar clefts and does not cycle to the clathrin-coated pit area and endosomes as occurs in other epithelia, including Caco-2 cells and OK cells (43). Nonetheless, we suggest that ClC-5 is serving the same function in exocytosis in both proximal tubule and OK cells, although the nature of that comportment has not been identified in either.

Concerning the mechanism by which reduced or absent ClC-5 reduces trafficking, it has been assumed that ClC-5, acting as a Cl^-/H^+ antiporter, neutralizes the electropositivity generated by the H^+-ATPase pumping H^+ ions into intracellular vesicles, thus allowing further acidification of the intracellular organelle in which both occur. Importantly, that this was the only role for ClC-5 was recently challenged by the demonstration of a role for Cl^- separate from charge neutralization as well as a role for intraorganellar cations in establishing intracellular organelle acid pH (22, 44). Of note, the identity of the intracellular organelle involved in NHE3 exocytosis has not been determined. Our results suggest that an NHE3-containing recycling endosome is likely to be affected by ClC-5 reduction.

As an alternative explanation to direct effects of ClC-5 on intracellular organelle function, because the NHERF multi-PDZ domain scaffolding proteins are known to be involved in inhibition of NHE3 by cAMP and Ca^{2+} and in dexamethasone stimulation (31, 41, 45, 46), it was determined whether there were any changes in the level of these proteins in the *Clcn5* KO. By immunoblots, there was no change in the amounts of NHERF1, -2, and -3 in *Clcn5* KO lysates of renal cortex (data not shown), indicating that changes in their levels did not account for abnormal Nhe3 activity in the *Clcn5* KO.

A surprising result of these studies was the apparently normal rate of both basal and stimulated NHE3 endocytosis in proximal tubule of both *Clcn5* KO and OK cells with ClC-5 expression knocked down. As reviewed above, there is strong evidence that multiple examples of endocytosis are ClC-5-dependent in renal proximal tubule, although many may be due to the reduced apical megalin and/or to the consequently elevated luminal PTH (2). However, there has recently been recognition that there are many forms of apical endocytosis in addition to receptor-mediated/clathrin-dependent and lipid raft-dependent forms. The mechanisms by which NHE3 is endocytosed have been shown to include clathrin-dependent and clathrin-independent forms, including via lipid rafts (47–49). Thus, it is possible that NHE3 endocytosis is not affected by reduced ClC-5, even though ClC-5 affects multiple forms of endocytosis, because NHE3 is taken up by some ClC-5-independent endocytic pathway(s).

In summary, these studies have established a role for ClC-5 in exocytosis of at least one renal proximal tubule apical membrane transporter (NHE3) as well as showing that although ClC-5 is necessary for multiple example of endocytosis it is not necessary for endocytosis of all proximal tubule proteins that are regulated partially by stimulated endocytosis. Demonstration of the importance of ClC-5 in the regulation of NHE3 trafficking should allow determination of the specificity of the dependence on ClC-5 in regulated exocytosis and endocytosis of additional apical proteins as well as providing a probe to isolate and identify the intracellular compartment in which ClC-5 is involved in NHE3 exocytosis.

Acknowledgments—We acknowledge the critical and helpful reading of this manuscript by Nicholas Zachos and Xuhang Li.

REFERENCES

1. Pook, M. A., Wrong, O., Wooding, C., Norden, A. G., Feest, T. G., and Thakker, R. V. (1993) *Hum. Mol. Genet.* **2,** 2129–2134
2. Piwon, N., Günther, W., Schwake, M., Bösl, M. R., and Jentsch, T. J. (2000) *Nature* **408,** 369–373
3. Wang, S. S., Devuyst, O., Courtoy, P. J., Wang, X. T., Wang, H., Wang, Y., Thakker, R. V., Guggino, S., and Guggino, W. B. (2000) *Hum. Mol. Genet.* **9,** 2937–2945
4. Cebotaru, V., Kaul, S., Devuyst, O., Cai, H., Racusen, L., Guggino, W. B., and Guggino, S. E. (2005) *Kidney Int.* **68,** 642–652
5. Guggino, S. E. (2007) *Nat. Clin. Pract. Nephrol.* **3,** 449–455
6. Fisher, S. E., Black, G. C., Lloyd, S. E., Hatchwell, E., Wrong, O., Thakker, R. V., and Craig, I. W. (1994) *Hum. Mol. Genet.* **3,** 2053–2059
7. Lloyd, S. E., Pearce, S. H., Günther, W., Kawaguchi, H., Igarashi, T., Jentsch, T. J., and Thakker, R. V.(1997) *J. Clin. Investig.* **99,** 967–974
8. Ludwig, M., Utsch, B., and Monnens, L. A. (2006) *Nephrol. Dial. Transplant.* **21,** 2708–2717
9. Dent, C. E., and Friedman, M. (1964) *Arch. Dis. Child* **39,** 240–249
10. Luyckx, V. A., Goda, F. O., Mount, D. B., Nishio, T., Hall, A., Hebert, S. C., Hammond, T. G., and Yu, A. S. (1998) *Am. J. Physiol. Renal Physiol.* **275,** F761–F769
11. Silva, I. V., Cebotaru, V., Wang, H., Wang, X. T., Wang, S. S., Guo, G., Devuyst, O., Thakker, R. V., Guggino, W. B., and Guggino, S. E. (2003) *J. Bone Miner. Res.* **18,** 615–623
12. Jentsch, T. J., Pusch, M., Rehfeldt, A., and Steinmeyer, K. (1993) *Ann. N.Y. Acad. Sci.* **707,** 285–293
13. Thiemann, A., Gründer, S., Pusch, M., and Jentsch, T. J. (1992) *Nature* **356,** 57–60
14. Zdebik, A. A., Zifarelli, G., Bergsdorf, E. Y., Soliani, P., Scheel, O., Jentsch, T. J., and Pusch, M. (2008) *J. Biol. Chem.* **283,** 4219–4227
15. Accardi, A., Walden, M., Nguitragool, W., Jayaram, H., Williams, C., and Miller, C. (2005) *J. Gen. Physiol.* **126,** 563–570
16. Scheel, O., Zdebik, A. A., Lourdel, S., and Jentsch, T. J. (2005) *Nature* **436,** 424–427
17. Devuyst, O., Christie, P. T., Courtoy, P. J., Beauwens, R., and Thakker, R. V. (1999) *Hum. Mol. Genet.* **8,** 247–257
18. Günther, W., Lüchow, A., Cluzeaud, F., Vandewalle, A., and Jentsch, T. J. (1998) *Proc. Natl. Acad. Sci. U.S.A.* **95,** 8075–8080
19. Hara-Chikuma, M., Wang, Y., Guggino, S. E., Guggino, W. B., and Verkman, A. S. (2005) *Biochem. Biophys. Res. Commun.* **329,** 941–946
20. Jentsch, T. J., Friedrich, T., Schriever, A., and Yamada, H. (1999) *Pflugers Arch.* **437,** 783–795
21. Günther, W., Piwon, N., and Jentsch, T. J. (2003) *Pflugers Arch.* **445,** 456–462
22. Novarino, G., Weinert, S., Rickheit, G., and Jentsch, T. J. (2010) *Science* **328,** 1398–1401
23. Christensen, E. I., Devuyst, O., Dom, G., Nielsen, R., Van der Smissen, P., Verroust, P., Leruth, M., Guggino, W. B., and Courtoy, P. J. (2003) *Proc. Natl. Acad. Sci. U.S.A.* **100,** 8472–8477
24. Yun, C. H., Oh, S., Zizak, M., Steplock, D., Tsao, S., Tse, C. M., Weinman, E. J., and Donowitz, M. (1997) *Proc. Natl. Acad. Sci. U.S.A.* **94,** 3010–3015
25. Murtazina, R., Kovbasnjuk, O., Zachos, N. C., Li, X., Chen, Y., Hubbard, A., Hogema, B. M., Steplock, D., Seidler, U., Hoque, K. M., Tse, C. M., De Jonge, H. R., Weinman, E. J., and Donowitz, M. (2007) *J. Biol. Chem.* **282,** 25141–25151
26. Levine, S. A., Nath, S. K., Yun, C. H., Yip, J. W., Montrose, M., Donowitz, M., and Tse, C. M. (1995) *J. Biol. Chem.* **270,** 13716–13725
27. Wang, T., Yang, C. L., Abbiati, T., Schultheis, P. J., Shull, G. E., Giebisch, G., and Aronson, P. S. (1999) *Am. J. Physiol. Renal. Physiol.* **277,** F298–F302
28. Hu, M. C., Fan, L., Crowder, L. A., Karim-Jimenez, Z., Murer, H., and Moe, O. W. (2001) *J. Biol. Chem.* **276,** 26906–26915
29. Sarker, R., Grønborg, M., Cha, B., Mohan, S., Chen, Y., Pandey, A., Litchfield, D., Donowitz, M., and Li, X. (2008) *Mol. Biol. Cell* **19,** 3859–3870
30. Collazo, R., Fan, L., Hu, M. C., Zhao, H., Wiederkehr, M. R., and Moe, O. W. (2000) *J. Biol. Chem.* **275,** 31601–31608
31. Bobulescu, I. A., Dwarakanath, V., Zou, L., Zhang, J., Baum, M., and Moe, O. W. (2005) *Am. J. Physiol. Renal Physiol.* **289,** F685–F691
32. Hryciw, D. H., Ekberg, J., Ferguson, C., Lee, A., Wang, D., Parton, R. G., Pollock, C. A., Yun, C. C., and Poronnik, P. (2006) *J. Biol. Chem.* **281,** 16068–16077
33. Yun, C. C., Chen, Y., and Lang, F. (2002) *J. Biol. Chem.* **277,** 7676–7683
34. Murer, H. (1992) *J. Am. Soc. Nephrol.* **2,** 1649–1965
35. Donowitz, M., and Li, X. (2007) *Physiol. Rev.* **87,** 825–872
36. Cavet, M. E., Akhter, S., Murtazina, R., Sanchez de Medina, F., Tse, C. M., and Donowitz, M. (2001) *Am. J. Physiol. Cell Physiol.* **281,** C2039–C2048
37. Wang, Y., Cai, H., Cebotaru, L., Hryciw, D. H., Weinman, E. J., Donowitz, M., Guggino, S. E., and Guggino, W. B. (2005) *Am. J. Physiol. Renal Physiol.* **289,** F850–F862
38. Bachmann, S., Schlichting, U., Geist, B., Mutig, K., Petsch, T., Bacic, D., Wagner, C. A., Kaissling, B., Biber, J., Murer, H., and Willnow, T. E. (2004) *J. Am. Soc. Nephrol.* **15,** 892–900
39. Bacic, D., Capuano, P., Gisler, S. M., Pribanic, S., Christensen, E. I., Biber, J., Loffing, J., Kaissling, B., Wagner, C. A., and Murer, H. (2003) *Pflugers Arch.* **446,** 475–484
40. Devuyst, O., Jouret, F., Auzanneau, C., and Courtoy, P. J. (2005) *Nephron Physiol.* **99,** p69–p73
41. Lee-Kwon, W., Kawano, K., Choi, J. W., Kim, J. H., and Donowitz, M. (2003) *J. Biol. Chem.* **278,** 16494–16501
42. Moulin, P., Igarashi, T., Van der Smissen, P., Cosyns, J. P., Verroust, P., Thakker, R. V., Scheinman, S. J., Courtoy, P. J., and Devuyst, O. (2003) *Kidney Int.* **63,** 1285–1295
43. McDonough, A. A., and Biemesderfer, D. (2003) *Curr. Opin. Nephrol. Hypertens.* **12,** 533–541
44. Steinberg, B. E., Huynh, K. K., Brodovitch, A., Jabs, S., Stauber, T., Jentsch,

T. J., and Grinstein, S. (2010) *J. Cell Biol.* **189,** 1171–1186
45. Cinar, A., Chen, M., Riederer, B., Bachmann, O., Wiemann, M., Manns, M., Kocher, O., and Seidler, U. (2007) *J. Physiol.* **581,** 1235–1246
46. Sarker, R., Valkhoff, V. E., Zachos, N. C., Lin, R., Cha, B., Chen, T. E., Guggino, S., Zizak, M., de Jonge, H., Hogema, B., and Donowitz, M. (2011) *Am. J. Physiol. Cell Physiol.* **300,** C771–C782
47. Li, X., Galli, T., Leu, S., Wade, J. B., Weinman, E. J., Leung, G., Cheong, A., Louvard, D., and Donowitz, M. (2001) *J. Physiol.* **537,** 537–552
48. Murtazina, R., Kovbasnjuk, O., Donowitz, M., and Li, X. (2006) *J. Biol. Chem.* **281,** 17845–17855
49. Chow, C. W., Khurana, S., Woodside, M., Grinstein, S., and Orlowski, J. (1999) *J. Biol. Chem.* **274,** 37551–37558